Power Plane Filter Using Higher Order Virtual Ground Fence

A. Ege Engin, *Member, IEEE*, Ivan Ndip, *Senior Member, IEEE*, Klaus-Dieter Lang, *Senior Member, IEEE*, and Gerardo Aguirre, *Senior Member, IEEE*

***Abstract*— The virtual ground fence (VGF) has been recently proposed to filter power plane noise in gigahertz frequency range. The VGF has distinct advantages over existing approaches, such as power islands and electromagnetic bandgap structures: The IR drop is not increased; transmission-line return-path discontinuities can be avoided; and the design procedure is simple. The basic VGF is created by using quarter-wave resonators referenced to the power or the ground plane. At the design frequency, the resonator creates an ac short circuit between the power and ground planes. An array of such resonators can be placed in electrically short intervals to create a VGF. Power plane noise will then ideally be shorted to ground at the location of the VGF. The operation principle is similar to the series resonance of a decoupling capacitor, which is usually ineffective in the gigahertz frequency range. This paper proposes a new design procedure for determining the number of quarter-wave resonators needed, their characteristic impedances, and their placement on the board. The design approach is based on the well-known insertion loss method in microwave filter theory, which allows for higher order VGF designs consisting of multiple rows of resonators.**

***Index Terms*— Materials characterization, power and ground planes, power distribution network, power integrity, simultaneous switching noise.**

I. Introduction

SIMULTANEOUS switching noise is a major bottleneck in designing robust electronic systems. The traditional approach to suppress noise generated by switching circuits is using decoupling capacitors. However, the equivalent series inductance of discrete capacitors and the inductance of vias used for mounting the capacitors make them unsuitable for providing noise isolation at higher frequencies than a few hundred megahertzes. This is especially a problem for analog/RF circuits sharing the same power supply as the noisy digital circuits.

Most packages and boards make use of power and ground planes in the power distribution network. This is a necessity for providing low IR drop and return paths for transmission lines. The power and ground planes carry not only the dc voltages, but also the switching noise across the board. Therefore, there has been great interest in filtering power plane noise [1]. A commonly used method is based on creating power islands that are connected to the rest of the power plane with a conducting bridge [2], [3]. Recently, periodic structures called electromagnetic bandgap (EBG) structures have been proposed to address power filtering of gigahertz switching noise [4]–[7]. An EBG structure looks like many power islands connected in a 2-D periodic pattern. Due to the narrow bridges connecting the power islands, these approaches require careful planning with regards to the IR drop and current return paths. The virtual ground fence (VGF) introduced in [8] does not suffer from IR drop or current return-path issues as it does not require patterning of the power plane, except a few via holes. The resonators can be designed as microstrip lines or striplines [9], or as semilumped elements [10].

Initial VGF designs were based on a single array of 50-Ω transmission lines behaving as quarter-wave resonators at the design frequency, which can be adjusted simply by changing the length of the resonators [8]. The higher order VGF has been introduced in [11], which can be considered as a 2-D quarter-wave open-circuit stub filter, as shown in Fig. 1.

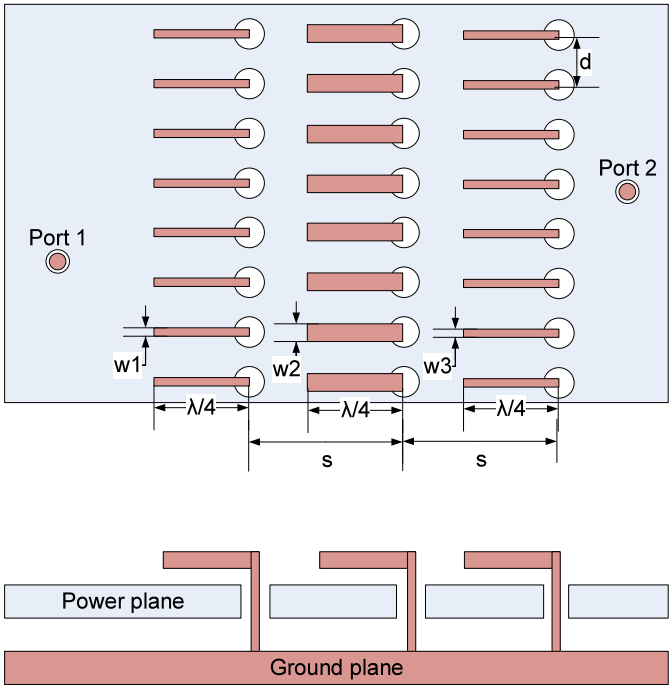

Fig. 1. Third-order VGF using microstrip resonators—top view and side view. The resonator widths and spacing are determined using microwave filter formulas.

Manuscript received August 15, 2016; revised November 21, 2016; accepted November 28, 2016. This work was supported in part by the National Science Foundation under Grant 1408637 and in part by the Alexander von Humboldt Foundation. Recommended for publication by Associate Editor S. Grivet-Talocia upon evaluation of reviewers' comments.

A. E. Engin is with the Department of Electrical and Computer Engineering, San Diego State University, San Diego, CA 92182 USA (e-mail: aengin@mail.sdsu.edu).

I. Ndip and K.-D. Lang are with the Fraunhofer-Institute for Reliability and Microintegration IZM, 13355 Berlin, Germany.

G. Aguirre is with Kyocera International, San Diego, CA 92111 USA.

Color versions of one or more of the figures in this paper are available online at http://ieeexplore.ieee.org.

Digital Object Identifier 10.1109/TCPMT.2016.2637300

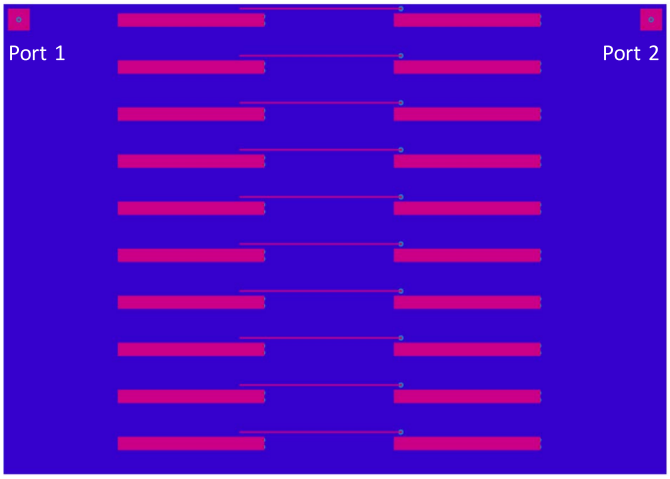

Fig. 2. Third-order VGF example. The resonators are designed to operate at 2 GHz.

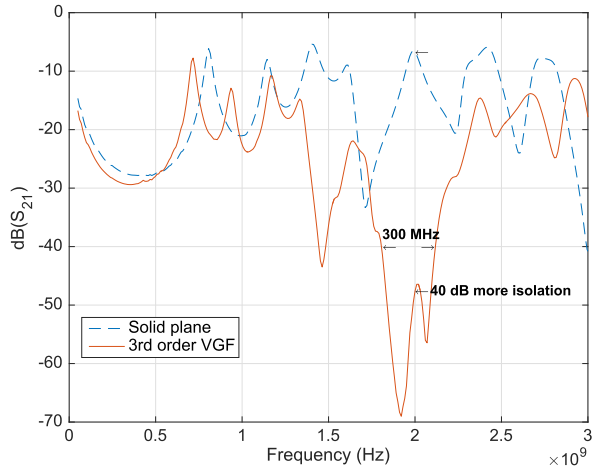

Fig. 3. Isolation is improved by 40 dB at the design frequency.

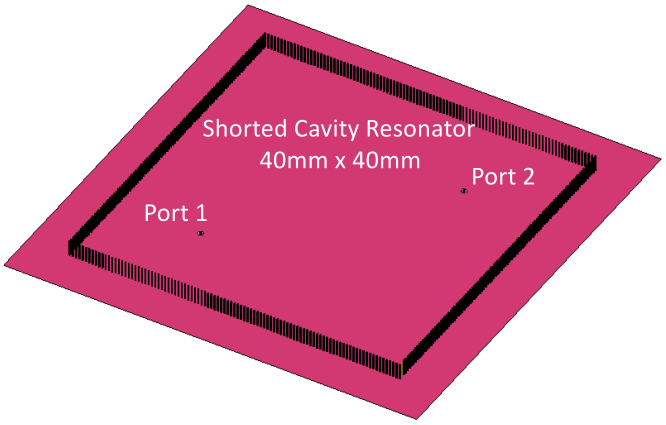

(a)

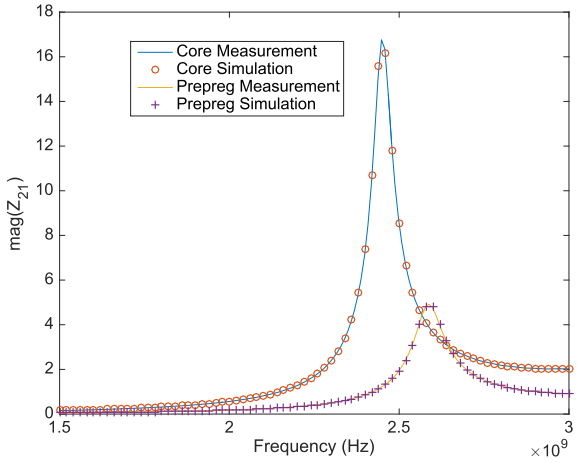

(b)

Fig. 4. (a) Shorted cavity resonators used to extract the dielectric thickness, loss tangent, and dielectric thickness. (b) Excellent match between simulation and measurement using the extracted parameters.

In this paper, we adopt this traditional filter design approach to VGF. However, we consider that a power filter does not require impedance matching unlike a traditional microwave filter. We study the dependence of VGF performance on several design options, such as the filter order, filter impedance, filter separation, board width, and board thickness. We also present a new methodology for accurate characterization of dielectric thickness, constant, and loss tangent for simulation to hardware correlation of VGF. Finally, a comparison to EBG structures is provided in terms of bandwidth and signal integrity impact.

II. Higher Order VGF Design Methodology

We design the VGF based on the common bandstop filter design approach using quarter-wave open-circuit stubs. In Fig. 1, a third-order filter implementation is shown as an example. This can be considered as a parallel connection of many bandstop filters. The open stubs in each row need to be placed in electrically short intervals so that $d \ll \lambda$. This ensures that plane waves between port 1 and port 2 need to go through the filter structure. Port 1 and port 2 can be considered as the location of a digital IC and RF/analog IC in a practical application.

The characteristic impedances of the stubs can be obtained using the formula

$$Z_{0n} = \frac{4Z_0}{\pi g_n \Delta} \tag{1}$$

where Z_{0n} is the characteristic impedance of the nth stub in a row, g_n is obtained from the table of prototype filter elements, and Δ is the fractional bandwidth of the filter. Z_0 would correspond to the characteristic impedance of the parallel-plate transmission-line section beneath the open stub. Z_0 would increase as the number of rows increases, so Z_0 is inversely proportional to d. To obtain a large fractional bandwidth Δ, small characteristic impedance Z_{0n} is desirable in addition to large Z_0.

All the stubs are quarter-wavelength, as shown in Fig. 1. Microstrip stubs with different widths will have different physical lengths due to the change in the effective dielectric constant. The separation s between each resonator also needs to be quarter-wavelength. Here, the wavelength would correspond to a signal between the power and ground planes. Hence, in general, stub lengths are going to be somewhat longer than the separation between the rows, if the same dielectric material is used in all layers in the board.

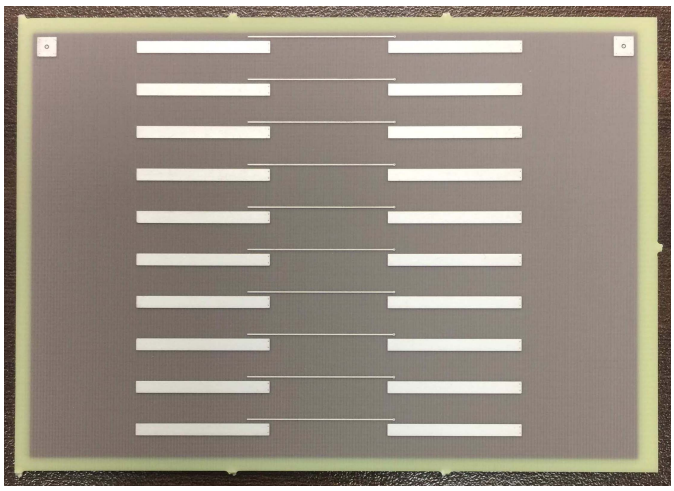

(a)

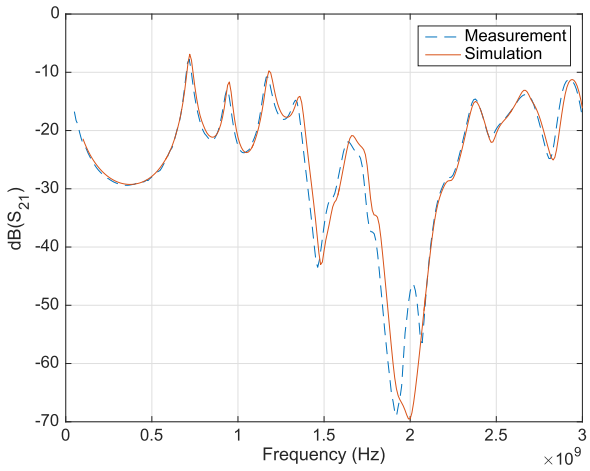

(b)

Fig. 5. (a) Picture of the test coupon for the third-order VGF. (b) Good simulation to hardware correlation.

The design procedure can then be summarized as follows.

1) Choose a prototype filter type and order (e.g., the third-order, 3-dB equiripple) to obtain g_n.
2) Choose d that satisfies $d \ll \lambda$. As a rule of thumb, $d = \lambda/10$ can be used.
3) Find the largest stub width w_n that can be realized on the board. Calculate the characteristic impedance Z_{0n} for that stub. All other characteristic impedances can then be obtained proportionally by properly scaling with the coefficients g_n.
4) Obtain all the stub lengths and separation s between the resonators as quarter-wavelength distances.

To illustrate the effectiveness of the VGF, test coupons have been measured and compared with a baseline board consisting of solid power and ground planes. The VGF design is based on a third-order 3-dB equiripple filter consisting of ten rows designed at 2 GHz. Top view of the 60 × 85.1-mm^2 layout is shown in Fig. 2. Two ports close to two top corners have been defined. Measurements were taken using microprobes.

Fig. 3 shows the improvement in isolation between port 1 and port 2 by 40 dB by introducing the higher order VGF

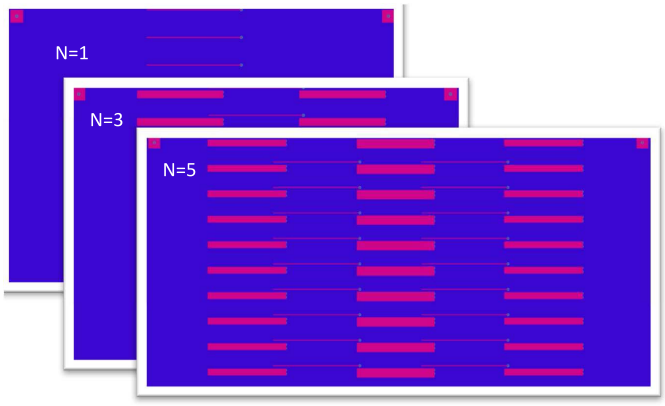

(a)

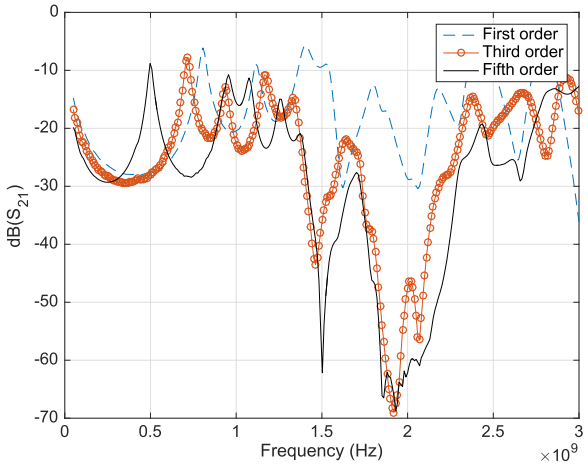

(b)

Fig. 6. (a) Layout of the first-, third-, and fifth-order VGF designs. (b) Higher order VGF improves both isolation level and bandwidth around the design frequency of 2 GHz.

at the design frequency. As an application example, an RF circuit at port 2 operating at 2 GHz would be isolated from the noise generated by a digital circuit at port 1. The bandwidth of the VGF is 300 MHz, if an absolute threshold value of 40-dB isolation is defined. By simply adjusting the lengths and spacings of the resonators, the design can be adjusted for a different operating frequency.

III. Simulation to Hardware Correlation

The measured boards consisted of a prepreg between microstrip stubs and power plane and a core substrate between the power plane and ground plane. The nominal thicknesses were 120 μm for the prepreg and 360 μm for the core. The board material is FR-4 with a nominal dielectric constant of 4.6 at 1 GHz as supplied by the board vendor. The loss tangent is not provided. To accommodate any deviations from the nominal values, it is important to extract the thickness, dielectric constant, as well as the loss tangent of the dielectrics. We designed simple shorted cavity resonators of size 40 × 40 mm^2 following the methodology in [12] and [13], as shown in Fig. 4. In this paper, we extended the automated extraction methodology in [13] by defining the dielectric thickness as one of the free variables as well.

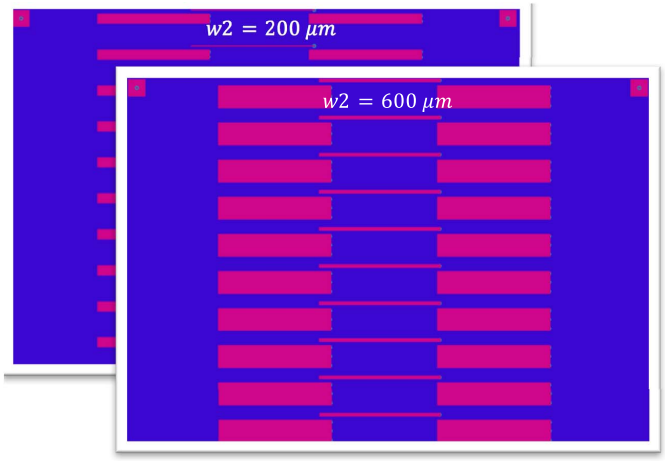

(a)

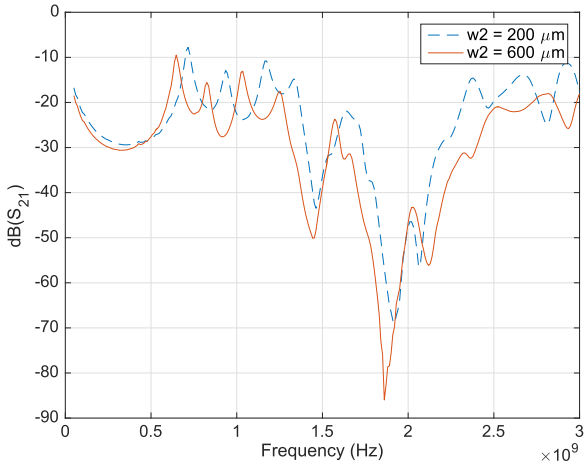

(b)

Fig. 7. (a) Layout of two VGF designs with different resonator characteristic impedances. (b) Lowering the resonator impedances by using wider traces improves VGF performance.

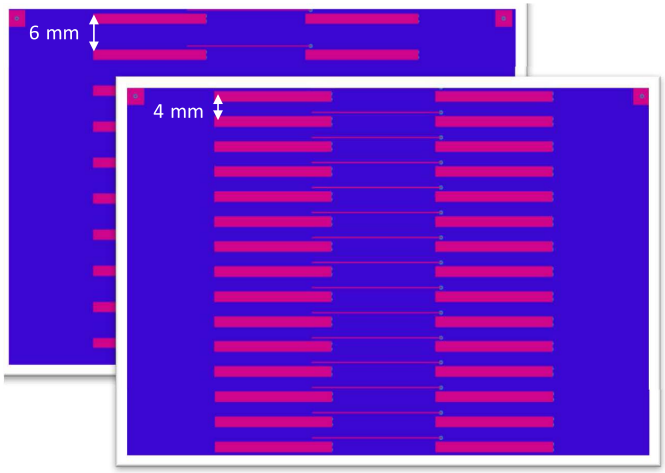

(a)

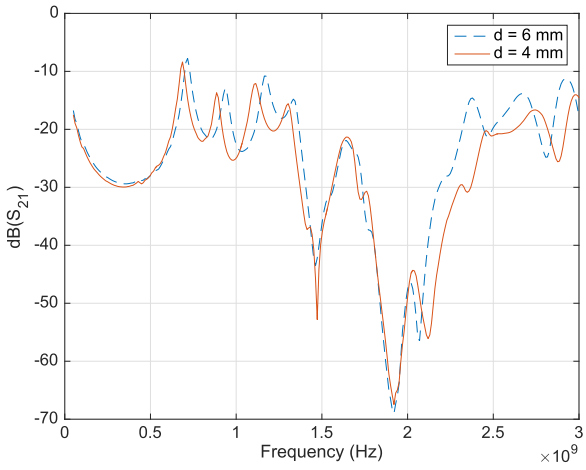

(b)

Fig. 8. (a) Layout of two VGF designs with different row separations. (b) Closer spaced rows increase the bandwidth of the filter.

The extracted parameters for the prepreg were the thickness of 153 μm, the dielectric constant of 4.16, and the loss tangent of 0.024. For the core layer, the same parameters were extracted as 371 μm, 4.66, and 0.018. Using the extracted parameters, the shorted cavity resonator was simulated using the full-wave simulator Sonnet [14]. Fig. 4 shows excellent match between the simulation and the measurement.

We apply the extracted parameters on the simulation of the VGF, as shown in Fig. 5. The good agreement indicates the accuracy of the extracted dielectric thickness, loss tangent, and dielectric thickness of the core and prepreg layers.

IV. Design Options for Higher Order VGF

The bandwidth and the level of isolation depend on several design options, such as the filter order, filter impedance, filter separation, board width, and board thickness in the VGF. In Sections IV-A–IV-E, we discuss the influence of these design options on the performance of the VGF.

A. Filter Order

Fig. 6 shows the effect of filter order on the VGF performance. The first-, third-, and fifth-order VGF designs are compared. It can be observed that a higher order VGF improves both isolation level and bandwidth. However, it requires more area possibly increasing the board size, as it was the case with the fifth-order VGF board.

B. Filter Impedance

Fig. 7 shows the effect of resonator characteristic impedance on the VGF performance. Two third-order VGF designs are compared to a middle resonator width of 200 and 600 μm. Other resonator widths are then scaled proportionally based on (1). It can be observed that lowering the resonator impedances by using wider traces improves VGF performance. However, the resonators cannot be made arbitrarily wide, as there should be room for signal traces to cross the board from one side of VGF to the other side.

C. Filter Separation

The VGF is based on periodically repeating a 1-D filter to fill a 2-D board. The distance d between each row needs to be electrically short to prevent any noise leakage across the VGF. Fig. 8 shows two cases where each 1-D filter occupies a width of 4 or 6 mm. The characteristic impedance Z_0 of the

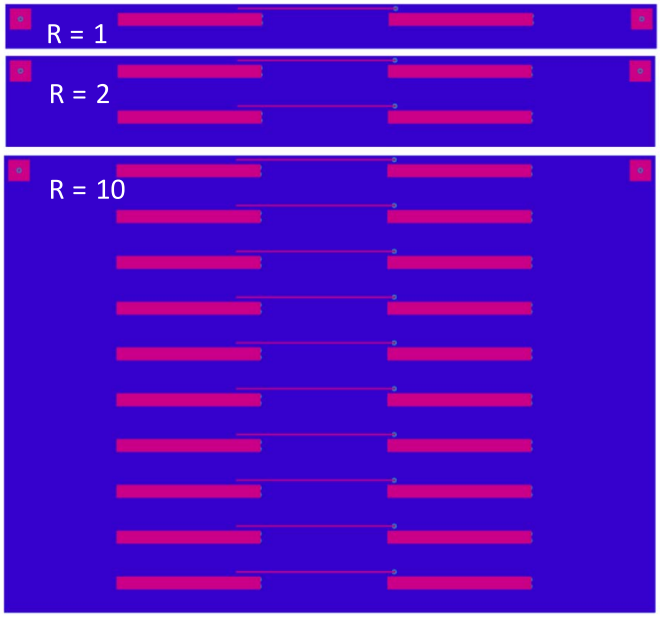

(a)

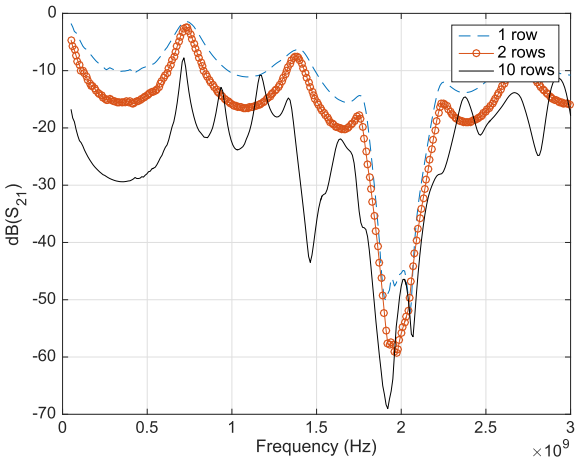

(b)

Fig. 9. (a) Three boards with different widths requiring one, two, and ten rows in VGF design. (b) VGF provides power filtering for all three cases at the design frequency of 2 GHz.

parallel-plate transmission line assigned to each row increases by using more rows. As Z_0 increases, the bandwidth Δ of the filter should increase following (1). Fig. 8 confirms the increase in bandwidth. Once again, there is a tradeoff with leaving room for signal traces.

D. Board Width

The VGF should provide power filtering for any board width. For narrower boards, a few rows of VGF should be sufficient. One example is shown in Fig. 9, where different board widths are studied, such that one, two, or ten rows of VGF were needed to fill the board. Fig. 9 shows that VGF provides power filtering for all three cases at the design frequency of 2 GHz.

E. Board Thickness

Varying the dielectric thickness between the power and ground planes would shift the bandgap frequencies of the

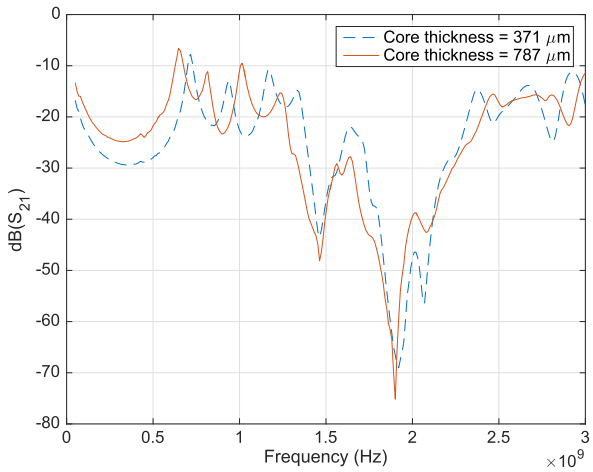

Fig. 10. Similar VGF design works for both thinner and thicker core between power and ground planes. VGF bandwidth is improved by using thicker core.

(a)

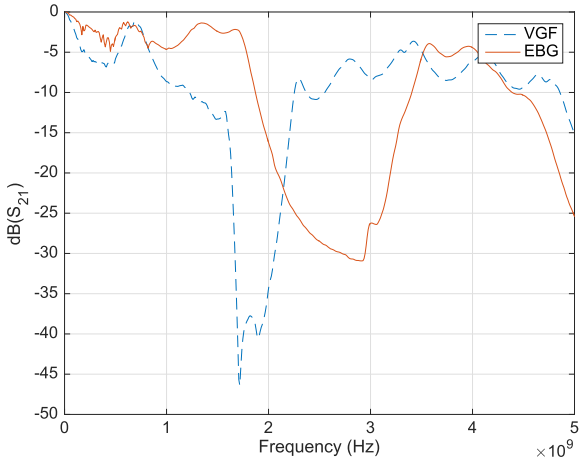

(b)

Fig. 11. (a) 1-D VGF versus EBG design. (b) Insertion loss.

conventional planar EBG structures. An advantage of the VGF is that the same design works for different dielectric thicknesses. A case is studied where the same VGF design in Fig. 2 is used on a board with a core thickness of 787 μm. The comparison to the thinner core of 371 μm is shown in Fig. 10. It can be seen that the VGF works also for the thicker core, and even with a better bandwidth. The characteristic impedance Z_0 of the parallel-plate transmission line assigned to each row increases by using thicker dielectrics. As Z_0 increases, the bandwidth Δ of the filter should increase following (1) as observed in Fig. 10.

V. Comparison With EBG Structures and Signal Integrity Consideration

Fig. 11 shows the comparison between a 1-D EBG structure and one-row VGF implemented on the thicker core of 787 μm.

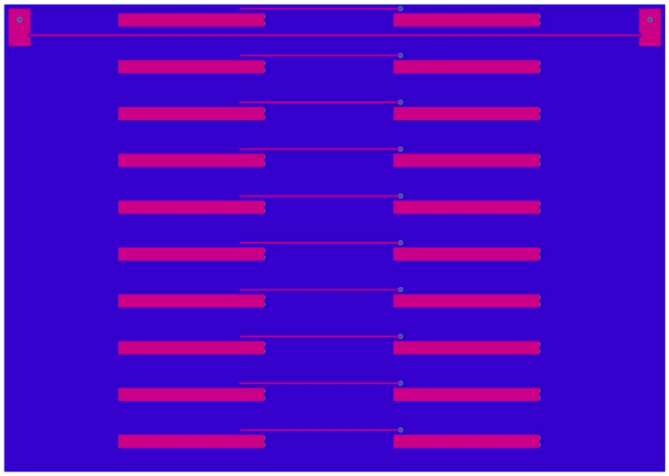

(a)

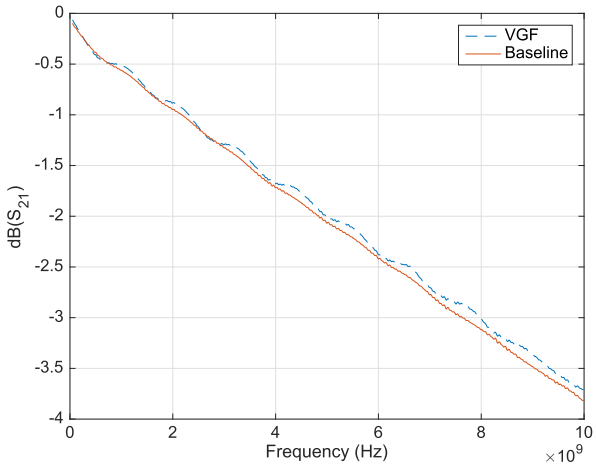

(b)

Fig. 12. (a) Single-ended microstripline routed between the rows of a VGF. (b) Insertion loss of the microstrip line is not increased by introducing the VGF.

The EBG structure does not address the same frequency range as the VGF. However, Fig. 11 shows that the bandwidth of the EBG structure is superior to the VGF for this example. This is expected, as the EBG is similar to a low-pass filter, whereas the VGF is based on a bandstop filter response. The bandwidth advantage of the EBG comes at an expense though. Due to the narrow bridges connecting the power islands, the IR drop is increased in the EBG, and the current return paths will be interrupted. To reduce the return-path issue, high-speed transmission lines with reference to planar EBG structures need to be routed as differential lines. This is not necessary in the VGF design as it does not create slits in the power plane. Therefore, IR drop is not increased, and the return current is not interrupted. As an example, Fig. 12(a) shows a single-ended microstrip line routed between the rows of a VGF. This is compared to a baseline board, where the VGF is removed. The insertion loss of the single-ended microstrip line is not degraded, as shown in Fig. 12(b), demonstrating the signal integrity advantage of the VGF.

VI. Conclusion

A new power plane filter design based on higher order VGF has been presented. Classical microwave filter design procedure has been extended to planar structures. The presented VGF has a simple design approach based on established microwave bandstop filter methodology, unlike the complicated planar EBG or power island designs that typically require electromagnetic simulations. In all studied cases, the VGF was able to provide isolation at the design frequency. Full-wave simulations confirm the accuracy of the measurements after careful extraction of dielectric thickness, constant, and loss tangent. The VGF requires minimal modifications on the existing power and ground planes, which, therefore, does not increase IR drop. It has also been shown that transmission lines have continuous return paths and the insertion loss is similar to a baseline board without VGF. Therefore, this new approach provides a robust methodology to provide power plane filtering in mixed-signal designs, which has not been possible with the existing power island or planar EBG designs.

References

[1] T.-L. Wu, H.-H. Chuang, and T.-K. Wang, "Overview of power integrity solutions on package and PCB: Decoupling and EBG isolation," *IEEE Trans. Electromagn. Compat.*, vol. 52, no. 2, pp. 346–356, May 2010.

[2] W. Cui, J. Fan, H. Shi, and J. L. Drewniak, "DC power bus noise isolation with power islands," in *Proc. IEEE Int. Symp. Electromagn. Compat. (EMC)*, vol. 2. Aug. 2001, pp. 899–903.

[3] A. E. Engin, "Efficient sensitivity calculations for optimization of power delivery network impedance," *IEEE Trans. Electromagn. Compat.*, vol. 52, no. 2, pp. 332–339, May 2010.

[4] M. Kim and D. G. Kam, "Wideband and compact EBG structure with balanced slots," *IEEE Trans. Compon., Packag., Manuf. Technol.*, vol. 5, no. 6, pp. 818–827, Jun. 2015.

[5] Y. Kasahara, H. Toyao, and T. Harada, "Open stub electromagnetic bandgap structure for 2.4/5.2 GHz dual-band suppression of power plane noise," in *Proc. IEEE Elect. Design Adv. Packag. Syst. Symp. (EDAPS)*, Dec. 2011, pp. 1–4.

[6] M. S. Zhang, Y. S. Li, C. Jia, and L. P. Li, "Simultaneous switching noise suppression in printed circuit boards using a compact 3-D cascaded electromagnetic-bandgap structure," *IEEE Trans. Microw. Theory Techn.*, vol. 55, no. 10, pp. 2200–2207, Oct. 2007.

[7] A. E. Engin, Y. Toyota, T. H. Kim, and M. Swaminathan, "Analysis and design of electromagnetic bandgap (EBG) structures for power plane isolation using 2D dispersion diagrams and scalability," in *Proc. IEEE Workshop Signal Propag. Interconnects*, Berlin, Germany, May 2006, pp. 79–82.

[8] A. E. Engin and J. Bowman, "Virtual ground fence for GHz power filtering on printed circuit boards," *IEEE Trans. Electromagn. Compat.*, vol. 55, no. 6, pp. 1277–1283, Dec. 2013.

[9] A. E. Engin and J. Bowman, "Virtual ground fence options for shielding power plane noise," in *Proc. IEEE Int. Symp. Electromagn. Compat. (EMC)*, Aug. 2014, pp. 460–464.

[10] M. Khorrami, "Optimized virtual ground fence for power delivery filtering of mixed-signal systems," in *Proc. IEEE Int. Symp. Electromagn. Compat. (EMC)*, Aug. 2014, pp. 346–350.

[11] A. E. Engin, I. Ndip, and K. D. Lang, "Higher-order virtual ground fence design for filtering power plane noise," in *Proc. 20th IEEE Workshop Signal Power Integr. (SPI)*, May 2016, pp. 1–3.

[12] A. E. Engin, "Extraction of dielectric constant and loss tangent using new rapid plane solver and analytical debye modeling for printed circuit boards," *IEEE Trans. Microw. Theory Techn.*, vol. 58, no. 1, pp. 211–219, Jan. 2010.

[13] A. E. Engin and P. Pasunoori, "Automated complex permittivity characterization of ceramic substrates considering surface-roughness loss," *J. Microelectron. Electron. Packag.*, vol. 9, pp. 144–148, Sep. 2012.

[14] Sonnet Softw. Inc., North Syracuse, NY, USA. *The Sonnet Suite User's Manual*, accessed on 2013. [Online]. Available: http://www.sonnetsoftware.com/

A. Ege Engin (M'05) received the B.S. degree in electrical engineering from Middle East Technical University, Ankara, Turkey, in 1998, the M.S. degree in electrical engineering from the University of Paderborn, Paderborn, Germany, in 2001, and the Ph.D. degree from the Leibniz University of Hannover, Hannover, Germany, in 2004.

He was a Research Engineer with the Fraunhofer-Institute for Reliability and Microintegration IZM, Berlin, Germany. From 2006 to 2008, he was an Assistant Research Director of the Microsystems Packaging Research Center, Georgia Institute of Technology, Atlanta, GA, USA. He is currently an Associate Professor with the Electrical and Computer Engineering Department, San Diego State University, San Diego, CA, USA. He has authored over 100 publications in journals and conferences in the areas of signal and power integrity modeling and simulation and has coauthored the book *Power Integrity Modeling and Design for Semiconductors and Systems (Prentice-Hall, 2008)*, translated to Japanese and Chinese. He holds four patents.

Dr. Engin was a recipient of the Semiconductor Research Corporation Inventor Recognition Award in 2009, the Outstanding Educator Award from the International Microelectronics Packaging and Assembly Society in 2015, and the Alexander-von-Humboldt Research Fellowship for 2015–2018.

Ivan Ndip (M'05–SM'12) received the M.Sc. and Ph.D. (*summa cum laude*) degrees (Hons.) in electrical engineering from the Technical University (TU) of Berlin, Berlin, Germany, in 2002 and 2006, respectively.

He joined the Fraunhofer-Institute for Reliability and Microintegration IZM, Berlin, as a Research Engineer in 2002. In 2005, he was the Group Manager of RF Modeling and Simulation and established the RF and High-Speed System Design Group at the Fraunhofer-Institute for Reliability and Microintegration IZM, and served as the Founding Group Manager until 2015. From 2005 to 2015, he built up and led a dynamic team of Research Engineers and Scientists and led the fundamental research projects and industrial Research and Development projects, with the national and international partners in the areas of measurement and analysis of dielectric materials in dependency on frequency and temperature, electromagnetic modeling, numerical simulation, measurement, and optimization of integrated antennas, high-frequency characterization and optimization of RF components, modules, and systems for signal/power integrity and intrasystem EMC, design of power-distribution networks and suppression of power-ground noise in mixed-signal modules, and RF system integration of transceiver modules. He has been a Lecturer with the School of Electrical Engineering and Computer Sciences, TU of Berlin, since 2008. Since 2014, he has been the Head of the Department of RF and Smart Sensor Systems, Fraunhofer-Institute for Reliability and Microintegration IZM. He also teaches professional development courses to practicing engineers and scientists worldwide. He has authored or coauthored over 150 publications in referred journals and conference proceedings.

Dr. Ndip is currently a member of the Technical Program Committee of many IEEE and the International Microelectronics Assembly and Packaging Society (IMAPS) international conferences. He is also a Fellow and a Life Member of IMAPS. He was a recipient of six best paper awards at leading international conferences and the Tiburtius-Prize, awarded yearly for outstanding Ph.D. dissertations in Berlin. He was also a recipient of the 2012 Fraunhofer IZM Research Award for his involvement in the development and successful application of novel methods, models, and design measures for electromagnetic optimization of high-frequency and high-speed systems, and the 2016 John A. Wagnon Technical Achievement Award for his outstanding technical contributions to the microelectronics industry worldwide. In 2013, he was the Technical Chair of the 46th International Symposium on Microelectronics in Orlando, FL, USA, and in 2014 he became the General Chair of the 47th International Symposium on Microelectronics, in San Diego, CA, USA. He also served as the General Chair of the 19th IEEE Workshop on Signal and Power Integrity 2015 in Berlin. He was a Technical Co-Chair of the 44th and 45th International Symposiums on Microelectronics in Long Beach, CA, USA, and San Diego, in 2011 and 2012, respectively. He chairs the Signal and Power Integrity Committee of the International Microelectronics Assembly and Packaging Society. He is an Associate Editor of the *Journal of Microelectronics and Electronic Packaging* and a Reviewer of the IEEE TRANSACTIONS ON ELECTROMAGNETIC COMPATIBILITY, the IEEE TRANSACTIONS ON COMPONENTS, PACKAGING, AND MANUFACTURING TECHNOLOGY, the IEEE TRANSACTIONS ON MICROWAVE THEORY AND TECHNIQUES, the IEEE TRANSACTIONS ON ELECTRON DEVICES, and other international journals.

Klaus-Dieter Lang (M'08–SM'13) received the M.Sc. (Dipl.Ing.) degree in electrical engineering and the Ph.D. degrees in wire bonding of multilayers and in quality assurance in assembly processes from the Humboldt University (HU) of Berlin, Berlin, Germany, in 1981, 1985, and 1989, respectively.

In 1981, he joined the HU of Berlin as a Researcher, where he was involved in microelectronic assembly, packaging, and quality assurance until 1991. In 1991, he joined SLV Hannover, Hannover, Germany, to build up a department for microelectronic and optic components manufacturing. In 1993, he became the Department Manager for Chip Interconnections, Fraunhofer Institute for Reliability and Microintegration IZM, Berlin, where he was the Director Personal Assistant from 1995 to 2000, and also responsible for Marketing and Public Relations. From 2001 to 2005, he coordinated the Branch Lab Microsystem Engineering, Adlershof, Germany. From 2003 to 2005, he was the Head of the Department Photonic and Power System Assembly and from 2006 to 2010 he has been the Deputy Director of the Fraunhofer-Institute for Reliability and Microintegration IZM. Since 2011, he has been the Director of the Fraunhofer-Institute for Reliability and Microintegration IZM and a Professor with the Technical University of Berlin, Berlin. He has authored or coauthored three books and over 130 publications in the field of wire bonding, microelectronic packaging, microsystems technologies, and chip on board.

Dr. Lang is currently a member of numerous scientific boards and conference committees, which include the Semiconductor Equipment and Materials International Award Committee, the Scientific Advisory Board of European Cluster of Electronic Packaging and Integration of Microdevices and Smart Systems, and the Executive Board of VDE-GMM. He is also a member of the Deutscher Verband für Schweißen und verwandte Verfahren e. V. and the International Microelectronic Assembly and Packaging Society, and plays an active role in the international packaging community as well as in conference organization. He is the Scientific Chair of the Conference Technologies of Printed Circuit Boards and SMT/HYBRID/PACKAGING.

Gerardo Aguirre (M'96–SM'14) was born in El Paso, TX, USA, in 1960. He received the B.S. degree from The University of Texas at El Paso, El Paso, in 1983, and the M.S. and Ph.D. degrees from The University of Arizona, Tucson, AZ, USA, in 1986 and 1996, respectively, all in electrical engineering.

He was with the Antenna Development Division, Radar Department, National Sandia Laboratories, Albuquerque, NM, USA, the Atmospheric Sciences Division, Los Alamos National Laboratories, Los Alamos, NM, USA and the Electronics Package Group, Texas Instruments, Dallas, TX, USA. His current research interests include electrical performance of electronic packages and high frequency properties of integrated circuit packages.

Dr. Aguirre is currently a Technical Staff Member with the Product Technology Center, Kyocera International, San Diego, CA, USA.